Case Studies in Thermal Engineering 79 (2026) 107783

Contents lists available at ScienceDirect

Case Studies in Thermal Engineering

journal homepage: www.elsevier.com/locate/csite

Experimental and thermodynamic analyses of a two-stroke UAV engine operated with gasoline–methanol blends

Erdal Tunçer

Istanbul Health and Technology University, Istanbul, Turkey

GRAPHICAL ABSTRACT

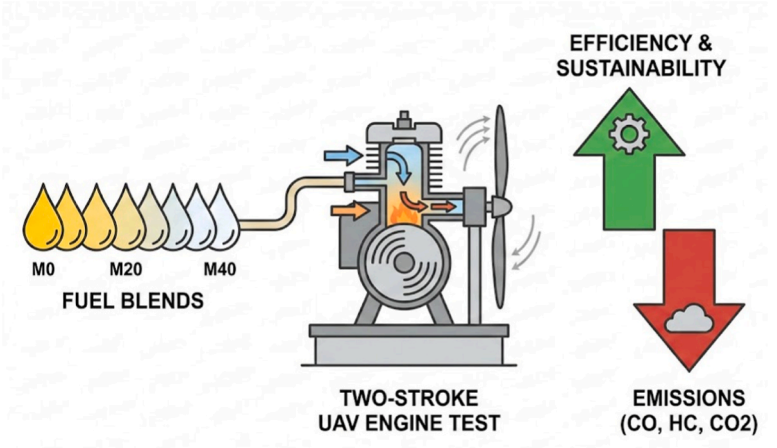

ARTICLE INFO

Keywords:
UAV engine
Methanol
Fuel
Energy
Exergy

ABSTRACT

This study delineates experimental investigations and thermodynamic analyses conducted on a two-cylinder, two-stroke, air-cooled engine-standard for uncrewed aerial vehicles (UAVs)-operated with various gasoline–methanol fuel blends. Performance and emission metrics were obtained at five thrust levels (5, 10, 15, 20, and 26 kg) utilizing five distinct fuel blends (M0, M10, M20, M30, and M40). The acquired data facilitated comprehensive evaluations of energy, exergy, and sustainability. At lower thrust levels, the minimal fuel consumption was observed with M0; at higher thrust levels, the minimum was recorded with M40. An increase in the methanol content within the fuel blends resulted in a notable reduction in CO_2 emissions; for instance, at a thrust of

E-mail address: erdal.tuncer@istun.edu.tr.

https://doi.org/10.1016/j.csite.2026.107783
Received 1 September 2025; Received in revised form 9 January 2026; Accepted 30 January 2026
Available online 6 February 2026

26 kg, CO_2 emissions were 5.65% for M0 and 3.91% for M40. The highest efficiencies in terms of energy and exergy were achieved at a thrust of 15 kg across all fuel blends. Correspondingly, the maximum sustainability index was determined to be 1.39 for M40 at a thrust of 15 kg.

1. Introduction

The ongoing increase in global energy demand, coupled with a predominant reliance on fossil fuels, raises considerable concerns regarding energy security and environmental sustainability. Scarcity of fossil reserves, price fluctuations, and adverse ecological impacts motivate the pursuit of alternative solutions, particularly within the transportation and aviation sectors [1]. The transportation sector remains a principal contributor to global carbon emissions, thereby exacerbating climate change and associated environmental challenges.

The rapid expansion of the Unmanned Aerial Vehicle (UAV) market has necessitated the search for more efficient and environmentally friendly propulsion systems [4]. While conventional gasoline engines are widely used in small-scale UAVs due to their high power-to-weight ratio, they suffer from relatively low thermal efficiency and high exhaust emissions. Consequently, researchers have focused on alternative fuels such as alcohols (ethanol, methanol), biodiesel, and hydrogen to improve combustion characteristics and reduce the environmental footprint of aviation engines. Alcohol-based fuels, in particular, have gained attention for spark-ignition (SI) engines due to their renewable nature and oxygenated structure, which promotes cleaner combustion [7,9].

Among alcohol fuels, methanol is considered a promising candidate for UAV applications. Methanol possesses a high octane number, which allows for higher compression ratios without knocking, thereby potentially increasing thermal efficiency [2]. Furthermore, the high latent heat of vaporization of methanol provides a significant cooling effect on the intake charge (charge cooling), increasing the volumetric efficiency and power density of the engine. However, methanol also has a lower lower heating value (LHV) compared to gasoline, which typically results in increased specific fuel consumption [8]. Several studies have investigated gasoline–methanol blends in automotive engines, reporting reductions in CO and HC emissions [10,24,31]; however, the specific application of these blends in two-stroke UAV engines and their impact on exergetic performance requires further detailed investigation. Apart from standard blends, researchers have also investigated various fuel additives such as nanoparticles [16] and different diesel-alcohol mixtures [17–19,23] to observe their effects on engine characteristics.

Despite technological advancements since the nineteenth century, internal combustion engines continue to play a central role in numerous energy conversion systems. Their high power-to-weight ratio, low capital costs, extensive engineering heritage, and relative ease of maintenance are critical factors contributing to their widespread utilization [2,3]. Although hybrid and electric propulsion systems are rapidly advancing, internal combustion engines remain the predominant power source in many mobility and aviation applications.

For uncrewed aerial vehicles (UAVs), internal combustion engines offer advantages such as extended endurance, rapid refuelling, low weight, and high energy density, rendering them attractive for various mission profiles [4]. Two-stroke piston engines, frequently employed in UAV applications, are preferred for their simple construction, high power-to-weight ratio, and cost-effectiveness. The operational flexibility provided by these engines is significant for reconnaissance, surveillance, and logistics missions.

Electric propulsion offers benefits including near-zero local emissions, low noise levels, and high efficiency; however, the limited energy density of batteries and range constraints restrict their applicability in long-duration or high-power UAV operations. Moreover, inadequate charging infrastructure and limited battery lifespan sustain the practical relevance of internal combustion engines for numerous UAV use cases [5].

Nonetheless, internal combustion engines face drawbacks such as relatively high fuel consumption, thermal management issues, vibration problems, and harmful exhaust emissions. Mitigating these adverse effects—especially in environmentally sensitive applications like UAVs—while maintaining or enhancing performance constitutes a critical research objective. Reducing fuel consumption offers operational advantages by decreasing take-off weight or increasing payload and endurance, which are vital considerations for UAV missions.

Alternative fuels have emerged as promising options. Alcohol-based fuels, particularly methanol and ethanol, are appealing due to their potential for renewable production, high octane number, low flame temperature, and intrinsic oxygen content, which can lead to improved combustion characteristics in internal combustion engines [6].

Methanol, in particular, possesses attributes of interest. Its high latent heat of vaporization and oxygen content promote more homogeneous mixture formation and stable combustion within the cylinder. These properties tend to reduce carbon monoxide (CO) and unburned hydrocarbon (HC) emissions while increasing knock resistance. Although methanol is toxic, it can be produced from biomass or natural gas, presenting a pathway towards potentially more sustainable fuel supply chains [7].

However, methanol's lower lower-heating-value (LHV) and high vaporization enthalpy may lead to increased fuel consumption when used in high fractions [8]. Therefore, identifying optimal methanol–gasoline blending ratios is essential for balancing performance and emissions.

A substantial body of literature has examined the effects of methanol–gasoline blends on engine performance and emissions. Many studies indicate that low-to-moderate methanol fractions (e.g., 10–30%) reduce CO and HC emissions, whereas higher fractions may result in efficiency losses and increased fuel consumption [9,10]. The impacts on nitrogen oxides (NOx) formation are mixed and appear to depend on operating conditions.

Most existing research focuses on automotive engines. However, studies addressing small-displacement, two-stroke, air-cooled

engines—particularly those used in UAVs—are scarce, and performance analyses based on energy and exergy are limited. This gap represents a significant deficiency both in scientific literature and practical applications.

Conventional energy analyses primarily evaluate engine performance through quantification of energy flows, but they do not account for irreversibilities or energy quality. Conversely, exergy analysis assesses the true available work potential of the fuel, enabling a more comprehensive evaluation of engine performance [11,17,24].

The sustainability index, an important extension of exergy analysis, serves as a crucial metric for aviation applications. Values exceeding one indicate sustainable operation. For UAV engines, this index reflects not only thermodynamic performance but also environmental and operational sustainability, making it a valuable indicator in the context of future aviation regulations (e.g., ICAO environmental standards, EURO 7).

Although thermodynamic analyses of internal combustion engines are widespread, exergy-based studies specifically targeting small-scale UAV engines remain limited. Among the few existing studies, Balli et al. [12] performed a comprehensive exergy analysis on a spark-ignition UAV engine (T620) and reported that the combustion process accounts for the highest exergy destruction, while exhaust losses represent the largest waste exergy stream. Similarly, Ozcan et al. [13] evaluated the environmental performance of a UAV engine and concluded that sustainability indicators improve significantly at higher engine loads due to reduced specific exergy destruction. In another study, Balli and Ozcan [14] integrated exergoeconomic and exergoenvironmental methods, highlighting that fuel cost is the dominant factor in the total cost of operation. Despite these valuable contributions, these studies have predominantly focused on standard gasoline. To the best of the authors' knowledge, there is no study in the literature that investigates the exergy and sustainability performance of a two-stroke UAV engine operated with gasoline–methanol blends. This study aims to fill this specific research gap.

This research endeavors to address the existing gap through experimental testing of gasoline–methanol blends (M0–M40) on a two-stroke, two-cylinder, air-cooled UAV engine. Performance and emission data were collected and utilized to perform energy and exergy analyses, assessing fuel exergy, exergy destruction, exergy efficiency, and sustainability indices.

The primary novelty of this work lies in its comprehensive assessment of methanol addition, encompassing not only energy and emissions but also exergy destruction and the sustainability index. The findings aim to provide direct guidance for alternative-fuel strategies for UAV engines and insights relevant to future aviation environmental regulations.

In conclusion, this study is among the inaugural efforts to evaluate the exergy-based performance of methanol–gasoline blends in UAV engines. The outcomes are expected to contribute to the scientific literature and facilitate the development of more sustainable and environmentally friendly propulsion systems for small-scale aviation.

2. Materials and methods

In this investigation, the test engine constitutes a commercially available model presently utilization in unmanned aerial vehicle (UAV) applications. From a technical perspective, the engine may be characterised as a two-cylinder, two-stroke, air-cooled, spark-ignition (SI) engine. The experimental procedures were conducted within a climate-controlled laboratory environment under stable ambient conditions (20 °C, 998 mbar, 52% relative humidity).

2.1. Test engine and technical specifications

The engine utilization in the experiments is produced by Erin Motor and is registered under the trade name Baykuş. Its technical specifications are detailed in Table 1. The engine has a maximum power output of 12 hp at 8000 rpm and is capable of producing a maximum static thrust of approximately 26 kg at sea level.

2.2. Test fuels

The fuels utilization in the experiments were procured from a local petroleum company. Pure gasoline was mixed with methanol (purity 99.5%) on a volumetric basis, and 2.5% synthetic lubricating oil (corresponding to a 40:1 ratio) was added to each blend to ensure proper lubrication of the engine components. The blend ratios and their respective codes are detailed in Table 2.

Table 1
Test engine specifications.

Producer	ERİN MOTOR A.Ş.
Brand/Model	BAYKUŞ/H12
Max. Engine Power	12 Hp
Max. Engine Speed	8000 rpm
Number of Strokes	2
Number of Cylinders	2
Fuel Injection Type	Carburettors
Stroke	36.5 mm
Bore	48 mm
Displacement	0.132 L
Compression Ratio	9.3
Ignition Advance	20° CA

Following preparation, all fuel blends were subjected to mixing in an ultrasonic stirrer operating at 50,000 Hz for 30 min, after which they were promptly tested in the engine. The physical and chemical characteristics of the blends are summarised in Table 3. The fundamental properties of the base fuels and their blends, including density, kinematic viscosity, and calorific value, were determined/verified in accordance with the ASTM D4052, ASTM D445,ASTM D93 and ASTM D240 standards, respectively, as specified in the table.

2.3. Experimental Setup

The experimental configuration is depicted in Fig. 1. The engine was mounted on a custom-designed floating test bed to isolate vibrations and allow for axial movement. The thrust force generated by the propeller was transferred via a horizontal linkage arm to an S-type load cell (SC516C) securely fixed to the static frame. The load cell, which was calibrated with standard weights prior to testing, continuously recorded the axial thrust force with a sensitivity of ±0.03 kg. The propeller used was a 26-inch fixed-pitch carbon fiber propeller optimized for UAV applications. Supplementary measurements encompass exhaust gas emissions, exhaust gas temperature, cylinder surface temperature, and fuel consumption. Finally, an uncertainty analysis was conducted in accordance with methodologies documented in the literature [39]. The measurement ranges, accuracies, and uncertainties of the sensors employed in the setup are detailed in Table 4.

2.4. Experimental procedure

The experiments were conducted at thrust forces of 5, 10, 15, 20, and 26 kg, which correspond to the stable operating ranges of the engine. At each thrust condition, measurements were taken for exhaust emissions, exhaust gas temperature, cylinder body temperature, and fuel consumption. Each test was performed three times, and the average values were utilization to generate the results and figures presented in this study.

The engine power was computed using the measured propeller diameter (26 inches), rotational speed, and thrust, employing the widely accepted propeller coefficient relations (Ct, Cp) documented in the literature. The specific fuel consumption (SFC) was subsequently calculated from the measured fuel flow and the computed power. Therefore, engine performance was assessed through the propeller test stand without the use of a dynamometer.

Fuel consumption was determined using a dual-verification approach to minimize experimental uncertainty. Both volumetric and gravimetric (mass-based) measurements were conducted simultaneously. The volumetric consumption was recorded using a graduated burette system and a stopwatch, while the mass depletion was monitored in real-time using a precision digital scale. The mass flow rate was calculated from the gravimetric data and cross-checked with the volumetric readings to ensure consistency. Regarding the engine operating conditions, the engine was not operated at a constant speed. Since the engine was coupled to a fixed-pitch propeller, the rotational speed was a dependent variable determined by the aerodynamic torque of the propeller at each throttle setting. Therefore, the experiments were controlled based on target thrust levels (5, 10, 15, 20, and 26 kg) rather than fixed engine speeds.

3. Thermodynamic analyses

This study encompasses both energy analysis, founded on the First Law of Thermodynamics, and exergy analysis, based on the Second Law. Additionally, the sustainability index was computed. The control volume employed in the analyses is depicted in Fig. 2.

The engine cylinder was defined as an open thermodynamic system (control volume). Since the process involves mass transfer (intake and exhaust) and a moving boundary (piston motion), the analysis considers the time-averaged steady-flow energy and exergy balance equations over a complete engine cycle, treating the engine as a steady-state open system for the overall performance evaluation. Ideal gas behaviour was assumed for all working fluids, and kinetic and potential energy changes were neglected. The reference environment for exergy calculations was taken as 20 °C and 1 atm. Steady-state conditions were assumed, and transient effects were neglected.

3.1. Energy analysis

The fundamental objective of all internal combustion engines is to produce useful work. Since the engine power was transferred directly to a propeller without a dynamometer, the effective power (P_{eff}) generated by the engine was calculated using the propeller thrust and rotational speed, based on the aerodynamic power coefficient (Cp) method commonly used in UAV applications:

Table 2
Fuel ratios and abbreviations.

Abbreviation	Gasoline (%)	Methanol (%)	Synthetic engine oil (%)
M0	100	0	2.5
M10	90	10	2.5
M20	80	20	2.5
M30	70	30	2.5
M40	60	40	2.5

Table 3
Fuel properties of test fuels.

Sample	Calorific Value (MJ/kg)	Density (@15°C) (kg/m^3)	Kinematic Viscosity (@40 °C) (mm2/s)	Flashpoint (°C)
M0	44.3	740	0.55	−45
M10	41.88	745	0.554	−45
M20	39.46	750	0.558	−45
M30	37.04	755	0.562	−45
M40	34.62	760	0.567	−45
Standard	ASTM D240	ASTM D4052	ASTM D445	ASTM D93

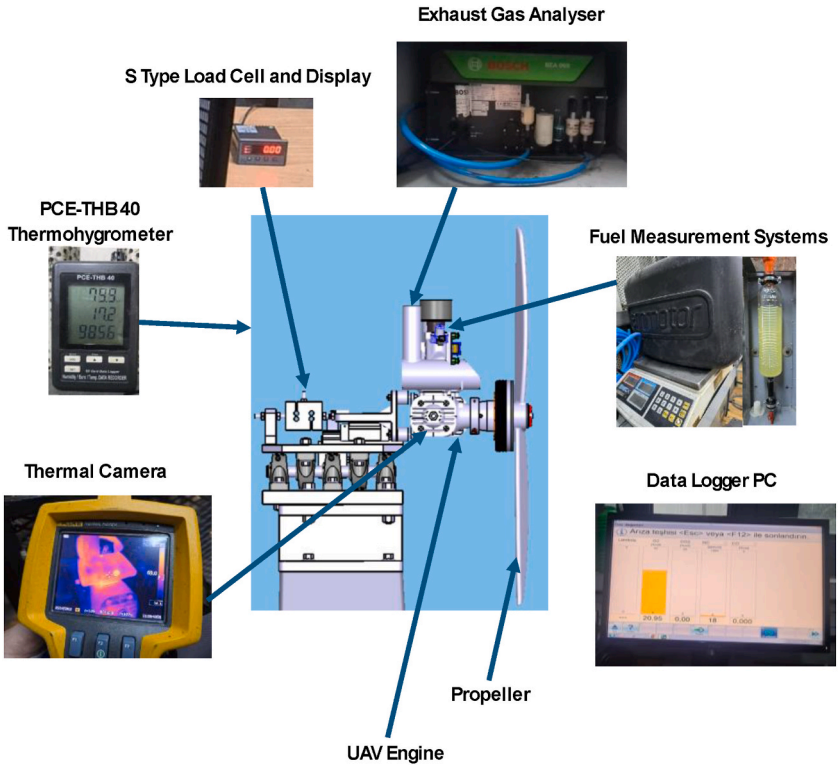

Fig. 1. Experimental setup.

Table 4
Measurement devices' accuracy and associated uncertainties.

Measured Parameter	Accuracy/ Sensitivity	Uncertainty/ Tolerance	Notes	Brand and Model
Shaft Speed (rpm)	1 rpm	±0.5%	Includes resolution and repeatability uncertainty	UNI-T UT372 Digital Laser tachometer
Thrust (kg)	±0.03 kg	±0.02 kg	Resolution and calibration-related uncertainty	Sensor-con SC516C Loadcell
Fuel Flow Time (s)	±0.1 s	±0.1 s	Chronometer precision	CASIO Hs-3v-1rdt Chronometer
Surface Temperature (°C)	±2 °C	-	Thermal camera accuracy	FLUKE TIS Thermal Camera
CO (%vol)	0.001%vol	±0.005%vol	Device sensitivity combined with tolerance	Bosch BEA 60 Gas Analyzer
CO_2 (%vol)	0.01%vol	±0.2%vol	Device sensitivity combined with tolerance	Bosch BEA 60 Gas Analyzer
HC (ppm vol)	1 ppm vol	±12 ppm	Device sensitivity combined with tolerance	Bosch BEA 60 Gas Analyzer
O_2 (%vol)	0.01%vol	±0.4%vol	Device sensitivity combined with tolerance	Bosch BEA 60 Gas Analyzer

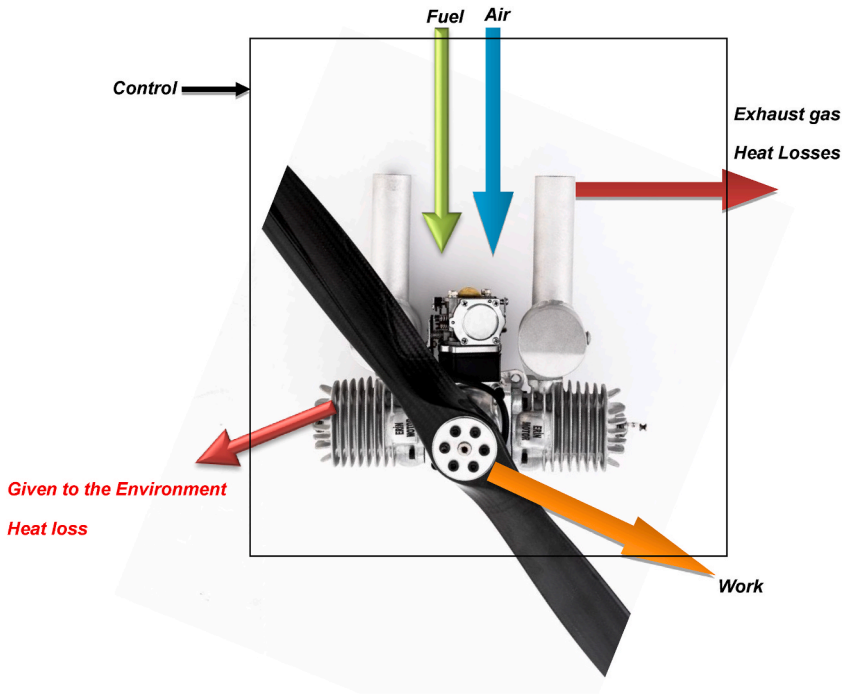

Fig. 2. Control volume used in thermodynamic analyses.

$$P_{eff} = \rho \cdot n^3 \cdot D^5 \cdot C_p \tag{1}$$

where ρ is the air density (kg/m3), n is the rotational speed (rev/s), D is the propeller diameter (m), and Cp is the dimensionless power coefficient. Specific fuel consumption (SFC), a critical performance metric, was calculated using the measured fuel mass flow rate and effective power:

$$SFC = \frac{\dot{m}_{fuel}}{P_{eff}} \times 3600 \tag{2}$$

Applying the first law of thermodynamics to the control volume illustrated in Fig. 2, the steady-flow energy balance equation can be expressed as:

$$\dot{Q}_{in} = \dot{W}_{net} + \dot{Q}_{loss} + \dot{H}_{exh} \tag{3}$$

The total energy input is primarily provided by the chemical energy of the fuel:

$$\dot{Q}_{in} = \dot{m}_{fuel} \cdot LHV_{fuel} \tag{4}$$

where $\dot{m}_{fuel}$ is the fuel mass flow rate (kg/s) and LHV_{fuel} is the lower heating value of the fuel (kJ/kg). The specific LHV values for each fuel blend used in the calculations are taken from the experimentally verified data presented in Table 3. The sensible enthalpy of the intake air was neglected as it enters at ambient reference conditions.

Finally, the thermal efficiency of the engine is defined as the ratio of useful work output to the fuel energy input:

$$\eta_{th} = \frac{P_{eff}}{\dot{Q}_{in}} \tag{5}$$

3.2. Exergy analysis

While energy analysis is crucial for assessing thermal efficiency, it does not account for the quality of energy. Exergy analysis, on the other hand, evaluates the maximum useful work obtainable from the fuel, thereby providing a more comprehensive performance indicator. The general exergy balance for the control volume is expressed in Equation (6) [20].

$$\dot{E}x_{air} + \dot{E}x_{fuel} = \dot{E}x_{w} + \dot{E}x_{ex} + \dot{E}x_{heat} + \dot{E}x_{dest} \tag{6}$$

Here, represents the exergy of the fuel ($\dot{E}x_{fuel}$), the exergy carried by exhaust gases ($\dot{E}x_{ex}$), the exergy of heat transferred from the engine

body ($\dot{E}x_{heat}$), and the exergy destruction ($\dot{E}x_{dest}$).

The exergy-based shaft power ($\dot{E}x_w$) represents the useful work output. Fuel exergy was calculated using the following empirical correlations [21]:

$$\dot{E}_{fuel} = \dot{m}_{fuel}\, \varphi LHV_{fuel} \tag{7}$$

The exergy factor (φ) was obtained using Equation (8) [22].

$$\varphi = 1.0401 + 0.1728\frac{h}{c} + 0.0432\frac{o}{c} + 0.2169\frac{\alpha}{c}\left(1 - 2.0628\frac{h}{c}\right) \tag{8}$$

Exhaust gas exergy was evaluated by first formulating the actual combustion reaction. The stoichiometric coefficients obtained from the combustion balance were used to determine exhaust gas mass flow. In this study, the total exhaust mass flow ($\dot{m}_{ex}$) was assumed to be 98% of the total mass flow entering the control volume. The specific exergy of the exhaust gas(ε_{ex}) is composed of physical (thermomechanical) and chemical exergy components:

$$\varepsilon_{e_x} = \varepsilon_{ph} + \varepsilon_{ch} \tag{9}$$

The total specific exergy of the exhaust gas is expressed as the sum of thermomechanical (physical) and chemical exergy components:

$$\psi_{exh} = \psi_{tm} + \psi_{ch} \tag{10}$$

The physical exergy component, assuming ideal gas behavior, is calculated using temperature and pressure differentials relative to the reference environment:

$$\varepsilon_{\{ph\}} = c_p[\,(T_{\{ex\}} - T_0) - T_0\, ln\,(\,\{T_{\{ex\}}\}/\{T_0\})] + R\,T_0\, ln\,(\,\{P_{\{ex\}}\}/\{P_0\}) \tag{11}$$

where cp is the specific heat capacity of the exhaust gas, R is the gas constant, and subscripts 'ex' and '0′ denote exhaust and environmental conditions, respectively. Since the exhaust discharges directly to the atmosphere, the pressure term ($P_{ex} \approx P_0$) is negligible.

The chemical exergy component is determined based on the molar composition of the exhaust species:

$$\varepsilon_{\{ch\}} = R\,T_0 \sum x_i\, ln\left(\frac{\{x_i\}}{\{y_i\}}\right) \tag{12}$$

In Equation (12), x_i represents the molar fraction of the i-th component in the exhaust gas, and y_i represents the molar fraction of the same component in the reference environment (atmosphere). The molar fractions of atmospheric gases were taken from literature data [25].

The exergy of heat transferred from the engine body to the environment was determined according to Equation (13) [26]:

$$\dot{E}x_{heat} = \sum\left(1 - \frac{T_0}{T_s}\right)\dot{Q}_{loss} \tag{13}$$

where Ts is the average surface temperature of the engine body, T_0 is the ambient temperature, and $\dot{Q}_{loss}$ is the rate of heat loss determined from the energy balance in Equation (3).

Entropy generation was evaluated using Equation (14) [27]:

$$\dot{s}_{gen} = \frac{\dot{E}x_{dest}}{T_0} \tag{14}$$

The exergy efficiency was finally obtained from Equation (15) [28]:

$$\eta_{ex} = \frac{\dot{E}x_W}{\dot{E}x_{in}} \tag{15}$$

3.3. Sustainability analysis

The sustainability index, derived from exergy efficiency, was calculated using Equation (16). For internal combustion engines, a sustainability index greater than one indicates acceptable sustainable operation [29].

$$\mathrm{SI} = \frac{1}{1 - \eta_{ex}} \tag{16}$$

4. Results and discussion

4.1. Fuel consumption

Fig. 3 demonstrates the variation in specific fuel consumption (SFC). The findings suggest that the incorporation of methanol into gasoline, as well as alterations in thrust load, considerably influence fuel consumption. The maximum fuel consumption was observed with the M40 blend at a thrust of 5 kg, whereas the minimum fuel consumption was recorded with pure gasoline (M0) at a thrust of 15 kg. As seen in Fig. 3, the specific fuel consumption (SFC) exhibits a non-linear trend with increasing thrust. The lowest SFC values were observed at the 15 kg thrust level for all fuel blends, indicating the engine's most efficient operating point (best efficiency point) in terms of thermal conversion. However, a significant change is observed as the thrust increases from 15 kg to 20 kg. In this range, the engine transitions from a partial-load cruise condition to a high-load regime. To maintain the required torque and cooling at higher loads (20 kg and above), the fuel metering system provides a richer mixture, leading to a noticeable increase in SFC. This effect is more pronounced in methanol blends due to their lower heating value, requiring a higher mass flow rate to satisfy the energy demand at high throttle openings.

This behavior is attributed to the physicochemical properties of methanol. Although methanol has a lower Lower Heating Value (LHV) than gasoline, its high latent heat of vaporization significantly lowers the intake charge temperature, increasing the air density and volumetric efficiency. Furthermore, at high thrust levels, air-cooled engines typically operate with richer gasoline mixtures to manage thermal loads. The cooling effect of methanol reduces the thermal strain, allowing for more efficient combustion without excessive enrichment. Additionally, the inherent oxygen content of methanol promotes complete combustion. These factors collectively compensate for the lower energy content, resulting in reduced fuel consumption at high loads compared to pure gasoline.

This behavior can be attributed to the lower heating value (approximately 20 MJ/kg) of methanol, which is nearly 50% lower than that of gasoline. The relatively modest decrease in power output is elucidated by methanol's high-octane number and lower latent heat of vaporization, which can partially enhance combustion within the cylinder and compensate for the loss in heating value. Prior studies have similarly indicated that the high latent heat of vaporization of methanol facilitates improved combustion efficiency compared to gasoline by diminishing the effective energy consumed within the cylinder. In this regard, the present study aligns with the existing literature [15].

4.2. Exhaust emissions

The analysis of carbon monoxide (CO) emissions at various load conditions, as presented in Fig. 4, demonstrates that the addition of methanol contributes to a reduction in CO formation across all thrust levels. Specifically, at lower loads ranging from 5 to 15 kg of thrust, CO concentration diminished from 2.97% with M0 to 1.42% with M40. This decline can primarily be attributed to the oxygenated characteristics of methanol, which enhance combustion efficiency and facilitate the complete oxidation of carbon to carbon dioxide (CO_2). Similar findings have been documented in existing literature, where methanol incorporation has been consistently associated with decreased CO emissions [9].

As the thrust increases to levels between 20 and 26 kg, a general escalation in CO emissions is observed, attributable to mixture enrichment, incomplete combustion processes, and higher in-cylinder temperatures at elevated loads. Nonetheless, even at a thrust level of 26 kg, significant reductions in CO levels are evident with methanol addition, decreasing from 7.0% with M0 to 3.20% with M40.

Overall, the lowest CO emissions were recorded with the M40 blend, indicating that higher methanol content is most effective in minimising CO formation. This observation is consistent with prior studies highlighting the CO reduction potential of methanol–gasoline blends [10].

The variation of NOx emissions with load, as depicted in Fig. 5, demonstrates irregular patterns at low and medium thrust levels,

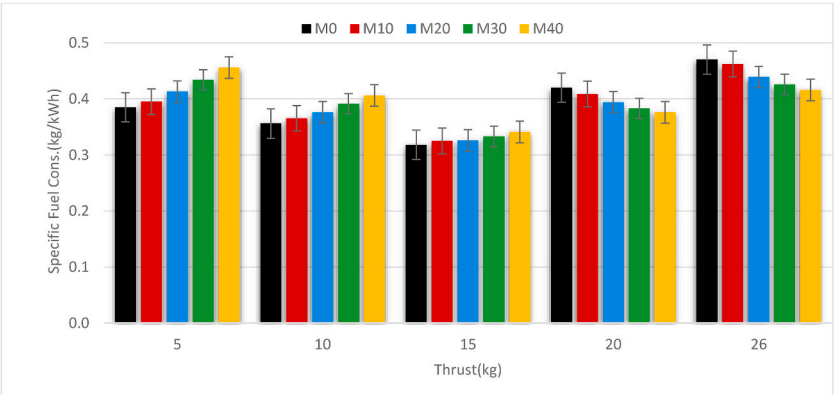

Fig. 3. Variation of specific fuel consumption (SFC) with thrust force for different fuel blends.

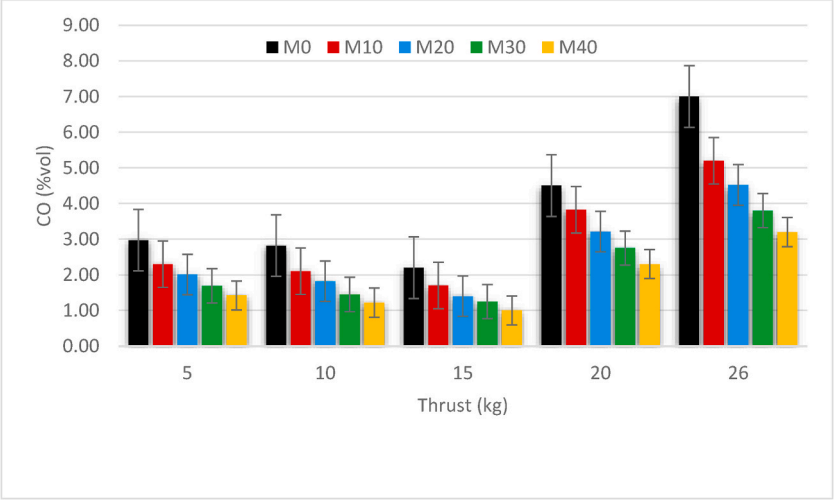

Fig. 4. Carbon monoxide (CO) emissions at various load conditions.

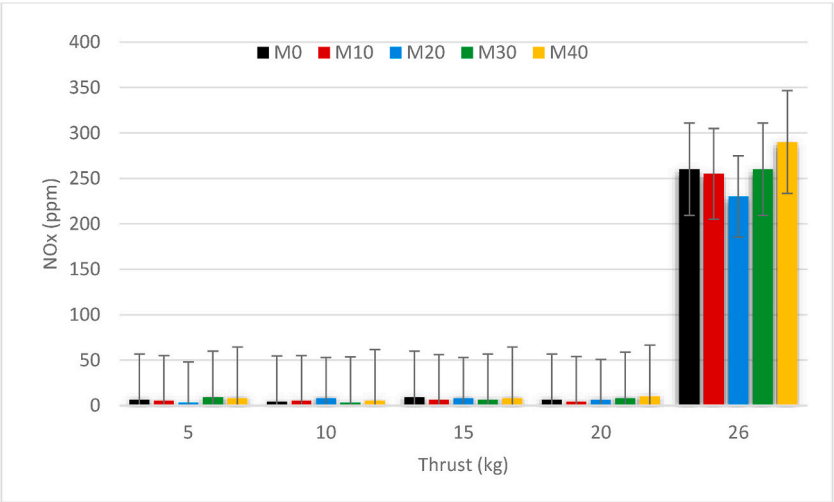

Fig. 5. Nitrogen Oxides (NOx) emissions at various load conditions.

with a pronounced increase observed at the highest load of 26 kg. This trend underscores the significant influence of combustion temperature on Nox formation. At lower loads, cylinder temperatures tend to be relatively low, resulting in limited NOx production ranging from 3 to 10 ppm. As the load increases, elevated combustion temperatures and pressures markedly elevate NOx levels, reaching between 230 and 290 ppm. These observations are consistent with existing literature, which indicates that NOx emissions tend to increase under high-load, high-temperature conditions [34].

The impact of methanol addition on NOx emissions exhibits complexity. At low and medium loads, no definitive reduction trend is apparent, likely attributable to variations in combustion characteristics and the air–fuel ratio. Conversely, at high loads, methanol content demonstrates a dual effect: at 26 kg thrust, NOx levels decrease from 260 ppm with M0 to 230 ppm with M20, before rising again to 290 ppm with M40. This suggests that moderate methanol concentrations can mitigate NOx emissions, whereas higher levels may elevate in-cylinder temperatures, thereby enhancing NOx formation. Similar findings have been reported by Huang et al. [10] and Verhelst [9]. Therefore, the optimal condition for minimising NOx emissions appears to be at intermediate methanol levels, such as M20.

To assess the thermal characteristics of the engine and their correlation with pollutant formation, the surface temperature of the exhaust muffler was monitored utilizing a thermal camera. The variation of surface temperature concerning thrust load is depicted in Fig. 6.

Although these values represent the external surface temperature rather than the temperature of gases within the cylinder, they serve as a valuable indicator of the comparative thermal load on the engine. As observed, the temperature generally increases with engine load. However, at low and medium thrust levels (5, 10, and 15 kg), the incorporation of methanol resulted in a conspicuous

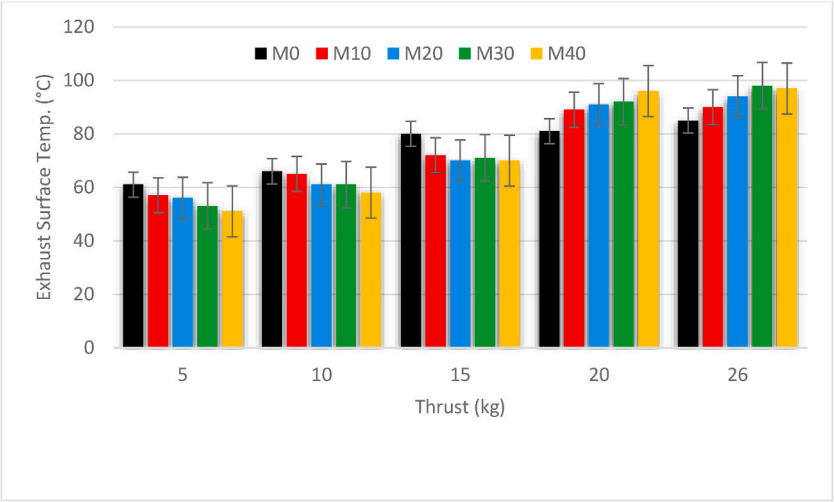

Fig. 6. Exhaust Surface Temperature at various load conditions.

reduction in surface temperature compared to pure gasoline (M0). For example, at 5 kg thrust, the temperature decreased from approximately 61 °C with M0 to 51 °C with M40. This cooling trend aligns with the high latent heat of vaporization of methanol, which absorbs significant heat during the intake and combustion processes.

While the surface temperatures at high loads (20 and 26 kg) displayed a converging trend between methanol blends and gasoline, the overall lower thermal profile at partial loads substantiates the findings concerning NOx emissions. Since NOx formation is strongly dependent on peak combustion temperatures, the observed cooling effect—even indirectly through surface measurements—contributes to explaining the suppressed NOx levels presented in Fig. 5.

The variation of HC emissions with load (Fig. 7) indicates higher levels at low loads. For instance, at 5 kg thrust, HC emissions were 3873 ppm with M0 and increased irregularly with methanol addition, reaching a maximum of 5650 ppm with M10. This trend can be attributed to methanol's high latent heat of vaporization, which reduces in-cylinder temperature and impairs mixture homogeneity under low-load conditions. Similar findings in the literature confirm that adding methanol can exacerbate HC emissions at light loads [31]. As load increases, HC emissions decrease substantially. This decline is primarily due to higher in-cylinder temperatures, which enhance combustion completeness. For example, at 15 kg thrust, HC emissions decreased from 2853 ppm with M0 to 1451 ppm with M30. At 26 kg thrust, HC emissions decreased from 5658 ppm (M0) to 2833 ppm (M30), effectively halving the emissions. These results confirm that methanol's oxygen content facilitates more complete combustion at medium and high loads. Similar reductions in HC emissions with alcohol addition have been extensively documented in the literature [9]. In conclusion, the optimal condition for HC emissions was achieved with M30, especially at medium and high loads. Nonetheless, the increase in HC emissions with M10 observed under low-load conditions highlights potential limitations during light-load operation.

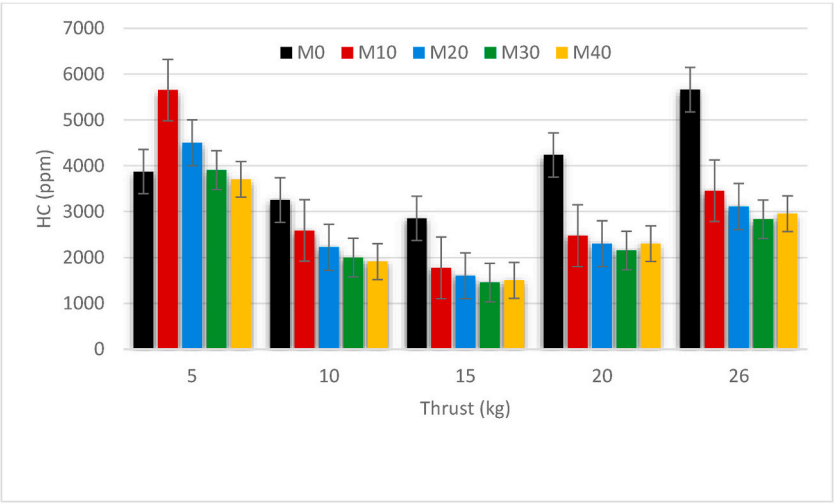

Fig. 7. Hydrocarbon (HC) emissions at various load conditions.

Carbon dioxide (CO_2) emissions serve as a significant indicator of the completeness of combustion. As illustrated in Fig. 8, CO_2 emissions exhibit a consistent increase with rising load, reflecting augmented fuel consumption and combustion efficiency at higher thrust levels. For instance, CO_2 emissions escalated from 1.29% at 5 kg thrust to 5.65% at 26 kg thrust for M0. This trend aligns with findings in the academic literature, which associate higher loads with increased CO_2 formation due to more complete combustion processes [35].

The addition of methanol, however, consistently resulted in a reduction of CO_2 emissions across all thrust levels. Specifically, at 15 kg thrust, CO_2 emissions decreased from 2.91% (M0) to 2.15% (M40). At 26 kg thrust, emissions declined from 5.65% (M0) to 3.91% (M40). This phenomenon can be attributed to methanol's lower carbon content and oxygenated structure, which facilitates lower CO_2 output. Similar reductions have been documented by Verhelst [9] and Huang et al. [10]. Consequently, the optimal condition for minimising CO_2 emissions was identified at the highest methanol content (M40).

4.3. Energy analysis

Based on fuel consumption data, the input fuel energy was calculated and is presented in Fig. 9. As expected, blends with higher heating values provided higher fuel energy. Among the tested fuels, M0 delivered the highest heating value at 44,300 kJ/kg, followed by M10 (41,880 kJ/kg), M20 (39,460 kJ/kg), M30 (37,040 kJ/kg), and M40 (34,620 kJ/kg). Consequently, fuel energy was consistently highest with M0 across all load conditions.

At a thrust level of 10 kg, the fuel energy was determined to be 22.78 kW for M0, 22.10 kW for M10, 21.43 kW for M20, 20.92 kW for M30, and 20.30 kW for M40. When operating at the maximum thrust of 26 kg, M0 produced 52.05 kW, whereas M40 generated only 36.00 kW. The relative difference between M0 and M40 was approximately 7.4% at a low load of 5 kg, increasing to 30.8% at a high load of 26 kg. This observation highlights the increasing influence of LHV at elevated loads. In summary, the addition of methanol resulted in a modest reduction in fuel energy at lower loads, while a more significant reduction was observed at higher loads. These findings are consistent with existing literature, which attributes the decreased energy output to methanol's lower LHV [36,37].

The results of thermal efficiency are illustrated in Fig. 10. The incorporation of methanol contributed to enhanced efficiency across all load conditions. For example, at a thrust of 5 kg, efficiencies were recorded as 21. 1% (M 0), 22. 1% (M 20), and 22. 8% (M 40). At a thrust of 15 kg, efficiencies reached 25. 5% (M 0), 27. 98% (M 20), and 30. 5% (M 40). At a thrust of 26 kg, efficiency improved from 17. 3% (M 0) to 25% (M 40). These enhancements are attributable to methanol' s oxygen content, which facilitates superior combustion, and its high latent heat, which diminishes knocking and permits more advanced ignition timing.

Methanol, owing to its intrinsic oxygen content, enhances combustion and contributes to the formation of a more homogeneous mixture within the cylinder. Additionally, its high latent heat of vaporization reduces temperatures within the combustion chamber, thereby decreasing the tendency for knocking and enabling the use of more advanced ignition timings. These properties, particularly under low and medium load conditions, lead to more efficient combustion, resulting in increased thermal efficiency. Specifically, within the thrust range of 5–15 kg, the improvement in thermal efficiency relative to M 0 was approximately 1–5%.

At higher loads, the tendency of gasoline to operate under rich mixture conditions, coupled with the associated increase in heat losses, reduces thermal efficiency. However, the addition of methanol helps to mitigate this decline. Notably, the M 40 blend demonstrated a distinct advantage, achieving a thermal efficiency of 25%, in comparison to gasoline operation. These findings are consistent with those reported in the literature. Sayin et al. [36] and Yilmaz et al. [37] emphasised that the oxygen content of methanol enhances thermal efficiency, while Tutak et al. [34] and Atmanli et al. [38] attributed the improvements in efficiency, particularly at medium loads, to methanol' s combustion characteristics and its high latent heat of vaporization. The obtained results showed

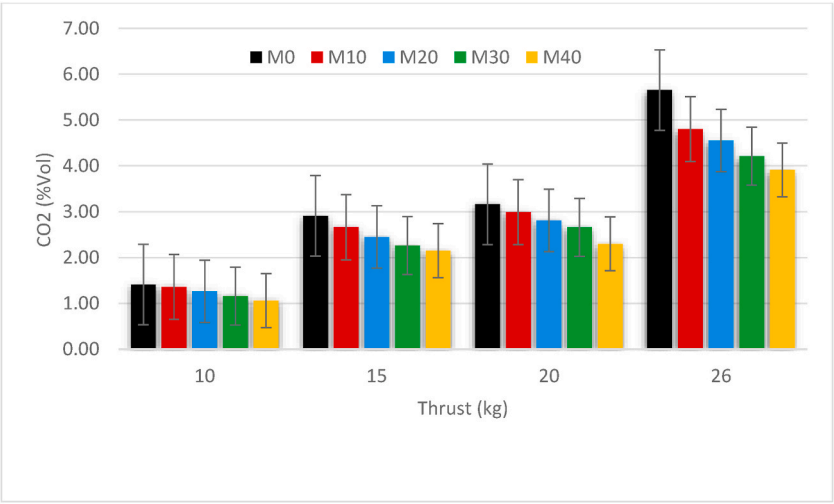

Fig. 8. Carbon dioxide (CO_2) emissions at various load conditions.

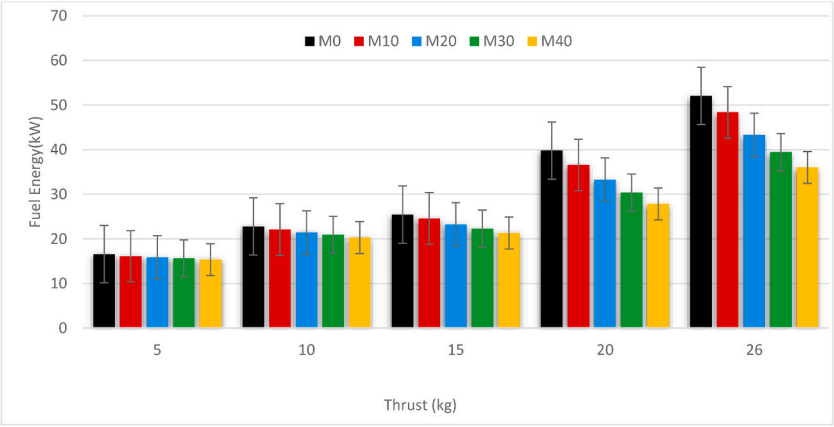

Fig. 9. Fuel energies at different thrust forces.

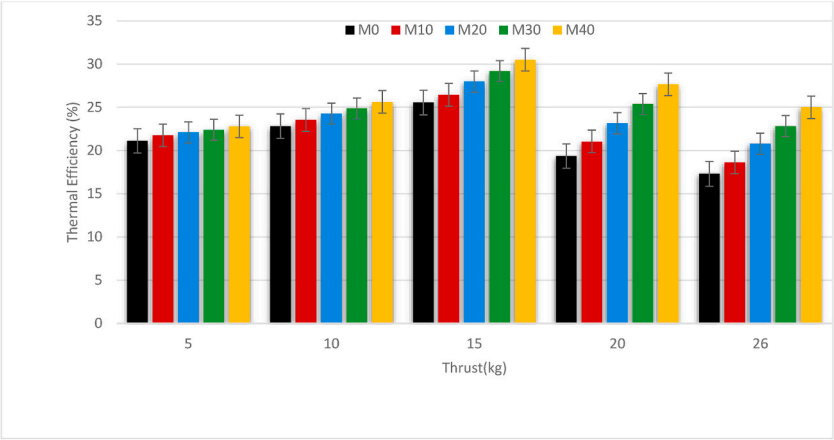

Fig. 10. Thermal efficiency at different thrust forces.

similarities with other studies in the literature [34,36–38].

4.4. *Exergy analysis*

This investigation involved the execution of an exergy analysis to determine the thermodynamic losses associated with gasoline–methanol fuel blends. The derived fuel exergy values are illustrated in Fig. 11. Upon review of the analysis results, it is evident that as thrust increases, the exergy values similarly rise, attributable to increased fuel consumption. At lower load conditions, the exergy values of the fuel blends demonstrate remarkable similarity; however, at higher loads, a significant decline in exergy values is observed

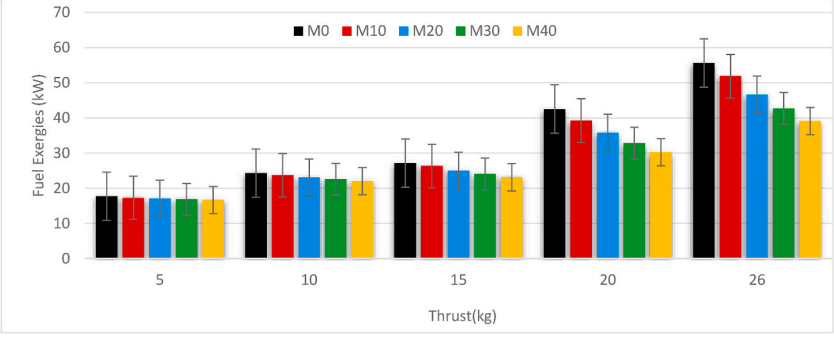

Fig. 11. Fuel exergies at different thrust forces.

concomitant with an increasing methanol ratio. For example, at thrust levels of 5 kg, 15 kg, and 26 kg, the M0 fuel produced 17.7 kW, 27.2 kW, and 55.6 kW of exergy, respectively. Under identical conditions, the M40 fuel produced 16.7 kW, 23.1 kW, and 39.1 kw. Consequently, the exergy of M0 fuel was found to be 5.6% higher at low load, 15.1% higher at medium load, and 29.7% higher at high load in comparison to M40 fuel.

The exergy of exhaust gases was calculated and is presented in Fig. 12. In internal combustion engines, the exergy of gases discharged into the atmosphere constitutes a loss of energy. An increase in exhaust exergy correlates with a decrease in engine efficiency. Consistent with existing literature, the efficient combustion of methanol ensures a reduction in exhaust exergy [11,33]. In this investigation, the addition of methanol to gasoline (M10, M20, and M30) was observed to decrease exhaust exergy. However, when the methanol content reached 40%, an increase in exhaust exergy was noted relative to M10, M20, and M30 fuels. For instance, at an output of 15 kg thrust, the exhaust exergy values for M0, M10, M20, M30, and M40 fuels were 1.463 kW, 1.412 kW, 1.375 kW, 1.363 kW, and 1.471 kW, respectively. At a thrust of 26 kg, the exhaust exergy values for these fuels were 2.965 kW, 2.836 kW, 2.767 kW, 2.703 kW, and 2.756 kW, respectively.

When the proportion of methanol ranged between 10% and 30%, combustion efficiency improved due to its oxygen content, resulting in a reduction of unburned gases and a consequent decrease in exhaust exergy. Conversely, at a methanol ratio of 40%, this trend was reversed, and an increase in exhaust exergy was observed. This phenomenon may be attributed to the increased difficulty in mixture formation at higher methanol proportions, disparities in flame propagation speed, and, particularly, in two-stroke engines, an increase in unburned fuel losses during scavenging. Furthermore, due to methanol's high latent heat of vaporization, in-cylinder temperatures may decline significantly, which can lead to incomplete combustion under full-load conditions and consequently increase the exergy carried away by the exhaust gases. This observation aligns with existing research concerning “combustion instability at high methanol fractions” [32].

Similar to exhaust exergy, the exergy of heat lost from the engine body to the atmosphere is also considered a loss. Thermal losses in engines adversely impact performance. In this study, the heat dissipated from the engine body to the atmosphere was quantified, and its exergy was subsequently determined, as presented in Fig. 13. At a thrust of 5 kg, the thermal exergy losses through the engine body were found to be comparable across all fuel blends (0.92–1.04 kW). However, as thrust increased, the disparities between the thermal exergies of the various fuel blends widened. For instance, at 10 kg thrust, the heat loss exergies for M0, M20, and M40 fuels were 1.46 kW, 1.32 kW, and 1.20 kW, respectively. At 26 kg thrust, the exergy of heat losses amounted to 3.93 kW, 3.04 kW, and 2.30 kW, respectively, for the same fuels. Enhancing the methanol ratio in the fuel blends results in a reduction of the exergy associated with thermal losses. For example, at 20 kg thrust, the exergy of heat losses for M0, M10, M20, M30, and M40 fuels were 2.87 kW, 2.54 kW, 2.20 kW, 1.90 kW, and 1.65 kW, respectively. An increase in methanol content results in a decrease in the thermal exergy lost from the engine body to the atmosphere. The primary rationale for this phenomenon is that, owing to methanol's high latent heat of vaporization, in-cylinder gas temperatures decrease, thereby reducing the temperature differential with the engine walls. This diminished temperature difference limits heat transfer and consequently reduces the energy and exergy losses through the engine body. Furthermore, the more uniform combustion facilitated by methanol suppresses local temperature peaks, thereby diminishing heat losses. Consequently, even at elevated thrust levels, the body heat loss associated with M40 fuel was significantly lower than that of M0. These findings align with existing literature indicating that methanol mitigates combustion chamber wall heat losses [30].

For fuels utilization in internal combustion engines, minimal exergy loss is advantageous because it signifies greater availability. Exergy destruction denotes the portion of fuel exergy that remains unutilized. Consequently, reducing exergy destruction positively influences engine performance enhancement. In the present study, the exergy destruction of fuel blends was quantified, and its variation across different thrust levels is depicted in Fig. 14. At lower thrust levels, the incorporation of methanol into the fuel blends did not produce a noticeable alteration in exergy destruction. Conversely, at higher thrust levels, exergy destruction exhibited a significant reduction upon the addition of methanol [11,33]. Specifically, at 20 kg thrust, the exergy destruction of the M40 fuel blend was 27.56% lower compared to that of the M0 fuel blend, while at 26 kg thrust, it was reduced by 26%. Increasing the methanol proportion in fuel blends contributes to a decrease in exergy destruction.

The primary reason for this reduction, particularly at higher loads, is the occurrence of more homogeneous and complete combustion. The oxygen content within methanol facilitates the in-cylinder oxidation reactions and diminishes unburned hydrocarbons. Moreover, due to its high latent heat of vaporization, a more balanced thermal profile within the combustion chamber prevents the formation of excessively high local hot spots, thereby reducing irreversibilities. Synthesising these effects, the useable energy portion of the fuel increases, resulting in decreased exergy destruction. However, since combustion stability tends to be more constrained at lower loads, the influence of methanol addition was not as pronounced. The results obtained are consistent with existing literature findings, which indicate that “methanol addition reduces exergy destruction at high loads” [32].

The exergy efficiencies of the fuel blends are depicted in Fig. 15. The peak exergy efficiency was attained at a thrust of 15 kg. At this thrust level, the exergy efficiencies for M0, M10, M20, M30, and M40 fuels were recorded as 23.92%, 24.65%, 25.98%, 26.99%, and 28.08%, respectively. At 20 kg and 26 kg thrusts, exergy efficiencies declined in comparison to the 15 kg thrust. It was observed that combustion losses increased as higher thrust was achieved. The augmentation of the methanol proportion in fuel blends resulted in increased exergy efficiency [11,33]. At 10 kg thrust, the exergy efficiencies of M0, M20, and M40 fuels were 21.37%, 22.53%, and 23.59%, respectively. For the same fuels at 26 kg thrust, the efficiencies were calculated as 16.18%, 19.29%, and 23.02%, respectively.

The reason for the highest exergy efficiency at 15 kg thrust is that the combustion efficiency reached its optimal level at this operating point. During medium loads, the air–fuel ratio is more balanced, and inadequate combustion alongside heat losses are minimised. Conversely, at higher loads (20–26 kg), increased cylinder temperatures lead to elevated heat losses and irreversibilities, along with a propensity for richer mixtures. This situation results in a reduction of exergy efficiency.

The enhancement of exergy efficiency with higher methanol ratios in fuel blends can be attributed to methanol's oxygen content,

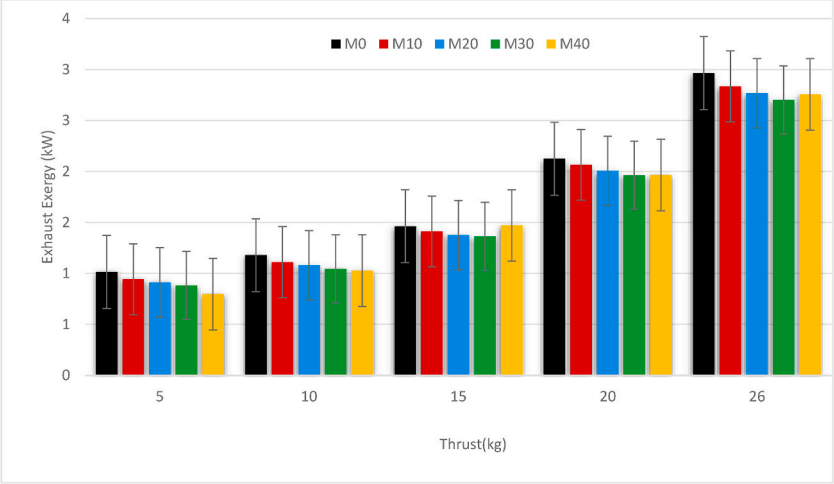

Fig. 12. Exhaust exergy change at different thrust forces.

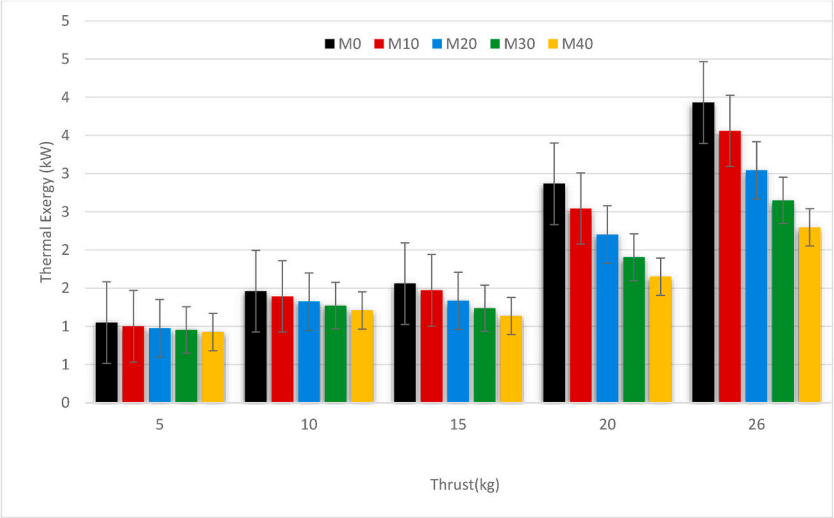

Fig. 13. Thermal exergy change at different thrust forces.

which facilitates more effective oxidation and diminishes unburned hydrocarbons. Furthermore, owing to methanol's high octane number, combustion becomes more stable, amplifying efficiency differences, particularly under high load conditions. For instance, at 26 kg thrust, the M40 fuel achieved an exergy efficiency of 23.02%, approximately 7% higher than M0. These findings corroborate the literature, which states that "methanol addition improves exergy efficiency at medium loads and limits the decline at high loads" [32].

4.5. Sustainability analysis

The sustainability index is a crucial parameter utilization in exergy analyses. This index must exceed 1. In this study, the sustainability indices were computed for various fuel blends and are depicted in Fig. 16. Consistent with exergy efficiency, the highest sustainability indices were observed at 15 kg thrust. This suggests that the engine operates most efficiently at this thrust level. At this point, the maximum sustainability index was calculated for the M40 fuel as 1.39. Similarly, at the same thrust, the sustainability indexes for M0, M10, M20, and M30 fuels were 1.31, 1.33, 1.35, and 1.37, respectively.

The occurrence of the highest sustainability index at 15 kg thrust indicates that the engine achieved its most balanced performance in terms of thermal and exergetic efficiency at this operating condition. At moderate loads, combustion stabilises more effectively, with heat losses and irreversibilities minimised. Consequently, exergy efficiency reaches its peak, and the sustainability index increases correspondingly.

The systematic increase in the methanol ratio correlates with a rise in the sustainability index. This is attributable to methanol's oxygen content, which facilitates cleaner and more efficient combustion, thereby reducing CO and HC emissions and enhancing the

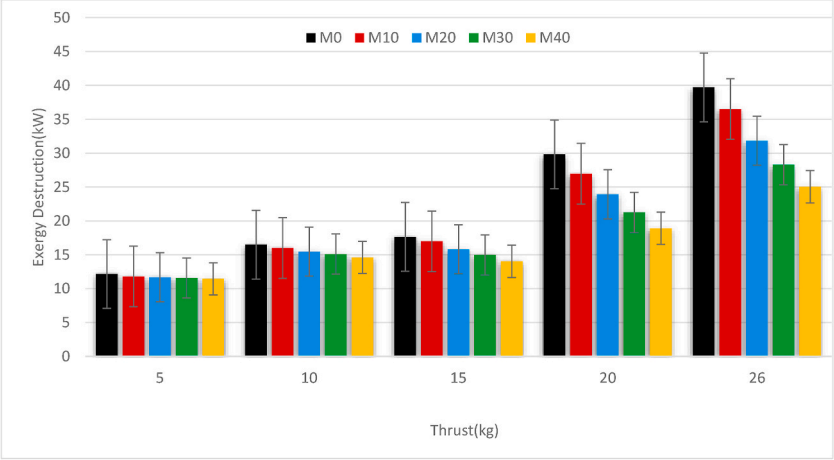

Fig. 14. Exergy destruction variation at different thrust forces.

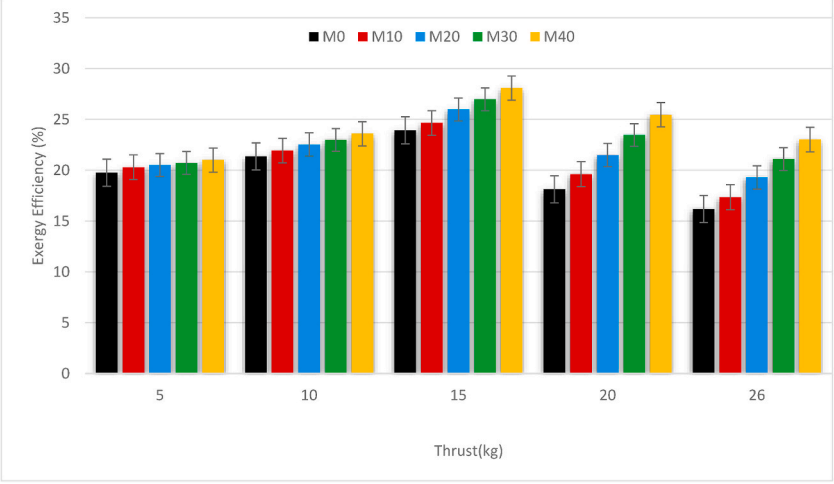

Fig. 15. Exergy efficiency at different thrust forces.

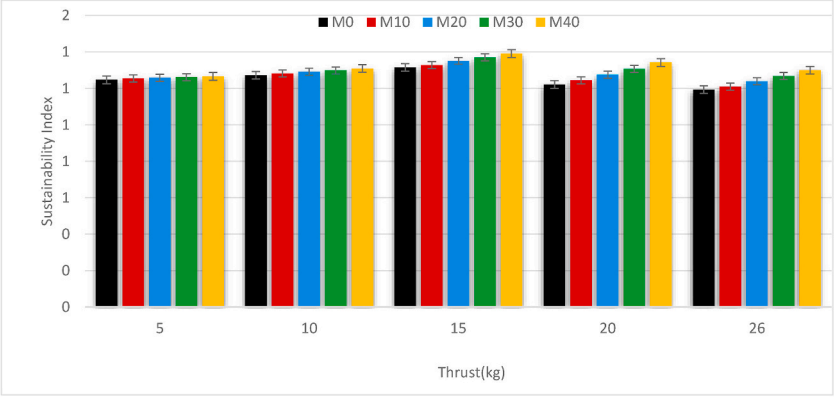

Fig. 16. Sustainability index in different driving forces.

useable fuel fraction. For instance, at 15 kg thrust, the M40 fuel attained a sustainability index of 1.39, approximately 6% higher than M0. This finding aligns with existing literature indicating that "oxygenated fuel additives improve both exergy efficiency and the sustainability index in engines" [11,33].

4.6. Limitations and future recommendations

While this study provides comprehensive insights into the exergetic performance of gasoline–methanol blends in UAV engines, it has certain limitations. First, the experiments were conducted under sea-level conditions. Since UAVs operate at various altitudes, the decrease in atmospheric pressure and air density at higher altitudes significantly impacts engine performance. As air density drops, the mass of oxygen available for combustion decreases, leading to a richer fuel-air mixture if not compensated. This phenomenon typically results in reduced volumetric efficiency, lower power output, and altered emission profiles compared to sea-level data. Therefore, the results presented here may differ under high-altitude flight conditions. Second, the engine performance was evaluated using a fixed-pitch propeller, which couples the engine speed directly to the thrust load. A dynamometer setup allowing for independent speed and load control could provide a broader map of engine behavior. Finally, the analysis assumed steady-state operation, neglecting the transient effects during rapid throttle changes common in UAV maneuvers.

Future research should focus on testing these fuel blends in an altitude chamber to simulate real-world flight conditions. Additionally, conducting in-flight tests with a UAV would provide valuable data on the practical applicability and transient response of methanol blends.

5. Conclusion and recommendations

This study comprehensively investigated the performance, emission characteristics, and exergetic sustainability of a two-stroke UAV engine fueled with gasoline–methanol blends (M0, M10, M20, M30, and M40) under various propeller thrust loads. The experimental data and thermodynamic analyses lead to the following key conclusions:

- Fuel Consumption and Efficiency: Fuel consumption exhibited notable variations depending on the engine thrust and methanol proportion. At a cruise thrust of 15 kg, the M40 blend showed a 6.77% increase in fuel consumption compared to pure gasoline (M0) due to its lower heating value. However, at a higher load of 26 kg thrust, M40 consumption decreased by 11.48%, indicating improved efficiency at high loads.
- Optimal Operating Range: The thermodynamic analysis identified the 15 kg thrust load as the engine's Best Efficiency Point (BEP). The maximum thermal efficiency was recorded as 30.49% with M40 fuel at this load, while the exergy efficiency reached 28.08% under the same conditions. This enhancement is attributed to the high octane number and improved combustion characteristics of methanol.
- Emission Reduction: Methanol addition significantly improved the environmental profile of the engine. A substantial reduction in CO_2 emissions was observed with increased methanol proportions; for instance, at 26 kg thrust, CO_2 emissions decreased from 5.65% with M10 to 3.91% with M40. This decline directly reflects the lower carbon content of methanol relative to gasoline.
- Thermal Management and Durability: Alcohol-based fuels produced cleaner combustion with less soot formation compared to pure gasoline. Additionally, the high latent heat of vaporization of methanol provided a cooling effect, which is beneficial for reducing thermal stress on the engine components and mitigating NOx formation.
- Strategic Advantage: The study confirms that alcohol-based fuels constitute an effective alternative for two-stroke UAV engines. The utilization of these fuels offers crucial benefits regarding compliance with environmental regulations and contributes to the reduction of the aviation sector's carbon footprint.

In conclusion, while methanol blends result in a slight penalty in volumetric fuel consumption at partial loads, they offer significant advantages in terms of thermal efficiency, power output, and emission reduction. Future work should focus on flight tests at varying altitudes and the development of optimized ECU maps to further capitalize on the properties of methanol.

Declaration of competing interest

The author declares that there are no known competing financial interests or personal relationships that could have appeared to influence the work reported in this manuscript. The experimental tests reported in this study were conducted at Erin Motor A.Ş. laboratories while the author was serving as R&D Manager. The author is currently no longer employed there but continues to provide consultancy services independently. This research did not receive any specific grant from funding agencies in the public, commercial, or not-for-profit sectors. The author confirms sole responsibility for the study design, data collection, analysis, and manuscript preparation.

Data availability

No data was used for the research described in the article.

References

[1] M.A. Rosen, I. Dincer, Exergy as the confluence of energy, environment and sustainable development, Exergy An Int. J. 1 (1) (2001) 3–13.
[2] J.B. Heywood, Internal Combustion Engine Fundamentals, second ed., McGraw-Hill Education, 2018.
[3] R. Stone, Introduction to Internal Combustion Engines, Palgrave Macmillan, 2012.
[4] Y. Feng, T. Chen, Q. Liu, H. Zhao, Adaptive speed control of a two-stroke engine with propeller for small UAVs based on scavenging measurement and modeling, Aerospace 12 (3) (2025) 202.
[5] B. Zhang, Z. Song, F. Zhao, L. Chunhua, Overview of propulsion systems for unmanned aerial vehicles, Energies 15 (2) (2022) 455.
[6] X. Zhen, Y. Wang, An overview of methanol as an internal combustion engine fuel, Renew. Sustain. Energy Rev. 52 (2015) 477–493.
[7] C.E. Montgomery, R.E. Sharp, Analysis of combustion characteristics and emissions of methanol–gasoline blends in spark ignition engines, Fuel 233 (2018) 374–381.
[8] H. Yaman, M.K. Yeşilyurt, S. Uslu, Determination of optimum methanol content for high performance and low emissions in spark ignition engines using response surface methodology, Fuel 304 (2021) 121403.
[9] S. Verhelst, Methanol as a fuel for internal combustion engines, in: International Conference on the Future of Automotive Fuels and Lubricants, 2019, pp. 1–16.
[10] J. Huang, H. Xiao, X. Yang, F. Guo, X. Hu, Effects of methanol blending on combustion characteristics and various emissions of a diesel engine fueled with soybean biodiesel, Fuel 285 (2020) 118734.
[11] D. Nir, Y. Singh, H. Sahu, S. Chauhan, Performance and exergy analysis of a two-stroke air-cooled engine operating with methanol-gasoline blends, J. Therm. Anal. Calorim. 146 (1) (2021) 127–138.
[12] O. Balli, H. Ozcan, H. Caliskan, Energy and exergy analyses of a gasoline fueled small-scale unmanned aerial vehicle engine, Energy Convers. Manag. 148 (2017) 1251–1260.
[13] H. Ozcan, O. Balli, H. Caliskan, Thermodynamic and environmental performance evaluation of a small-scale unmanned aerial vehicle engine, Energy Rep. 7 (2021) 345–356.
[14] O. Balli, H. Ozcan, Exergoeconomic and exergoenvironmental analyses of a small-scale gasoline fueled unmanned aerial vehicle engine, Energy Convers. Manag. 178 (2018) 203–214.
[15] M. Alramadan, A. Al-Hassani, S. Naji, A review of the effects of methanol–gasoline blends on the performance and emissions of spark ignition engines, J. Eng. Sci. Technol. 15 (4) (2020) 2187–2199.
[16] B. Doğan, M.K. Yeşilyurt, H. Yaman, N. Korkmaz, A. Arslan, Green synthesis of SiO2 and TiO2 nanoparticles using safflower (Carthamus tinctorius L.) leaves and investigation of their usability as alternative fuel additives for diesel-safflower oil biodiesel blends, Fuel 367 (2024) 131498.
[17] T. Akbiyik, N. Kahraman, T. Taner, Energy and exergy analysis with emissions evaluation of a gasoline engine using different fuels, Fuel 345 (2023) 128189.
[18] İ. Örs, S. Yelbey, H.E. Gülcan, B.S. Kul, M. Ciniviz, Evaluation of detailed combustion, energy and exergy analysis on ethanol-gasoline and methanol-gasoline blends of a spark ignition engine, Fuel 354 (2023) 129340.
[19] H. Feng, X. Chen, L. Sun, R. Ma, X. Zhang, L. Zhu, C. Yang, The effect of methanol/diesel fuel blends with co-solvent on diesel engine combustion based on experiment and exergy analysis, Energy 282 (2023) 128792.
[20] B. Ma, Q. Zhan, A. Yao, C. Yao, Exergy analysis of a diesel methanol dual fuel engine with different regulatory strategies for meeting China VI emission regulations, Case Stud. Therm. Eng. 63 (2024) 105350.
[21] S.K. Gupta, K.A. Subramanian, Energy and exergy analysis of the automotive spark-ignition engine fueled with ethanol, methanol, and gasoline, in: International Conference on Recent Advances in Materials, Manufacturing and Thermal Engineering, Springer Nature Singapore, Singapore, 2022, July, pp. 525–533.
[22] M. Djermouni, A. Ouadha, Thermodynamic analysis of methanol, ammonia, and hydrogen as alternative fuels in HCCI engines, Int. J. Thermofluids 19 (2023) 100372.
[23] S. Allahyari, F. Mohammadkhani, M. Yari, Combustion and exergy investigation of a compression ignition engine fueled with ethanol and methanol blends, Energy Equip. Syst. 9 (2) (2021) 159–172.
[24] S. Lee, Y. Kim, J. Lee, K. Kim, S. Lee, K. Min, S. Oh, Energy and exergy analyses of hydrogen-fueled spark ignition engine with various air excess ratios and ignition timings, Fuel 349 (2023) 128588.
[25] B. Doğan, D. Erol, The investigation of energy and exergy analyses in compression ignition engines using diesel/biodiesel fuel blends-a review, J. Therm. Anal. Calorim. 148 (5) (2023) 1765–1782.
[26] C.H. Rufino, A.J. de Lima, A.P. Mattos, F.U. Allah, J.L. Bernal, J.V. Ferreira, W.L. Gallo, Exergetic analysis of a spark ignition engine fuelled with ethanol, Energy Convers. Manag. 192 (2019) 20–29.
[27] B. Dogan, A. Cakmak, M.K. Yesilyurt, D. Erol, Investigation on 1-heptanol as an oxygenated additive with diesel fuel for compression-ignition engine applications: an approach in terms of energy, exergy, exergoeconomic, enviroeconomic, and sustainability analyses, Fuel 275 (2020) 117973.
[28] E. Tunçer, B. Doğan, T. Sandalcı, D. Erol, Energy and exergy analyses of skipped cycle mode in a single-cylinder engine fuelled with diesel and natural gas, Int. J. Exergy 39 (2) (2022) 173–194.
[29] S. Sarıkoç, İ. Örs, S. Ünalan, An experimental study on energy-exergy analysis and sustainability index in a diesel engine with direct injection diesel-biodiesel-butanol fuel blends, Fuel 268 (2020) 117321.
[30] M. Hussain, Z. Ma, S. Liu, M.I. Khan, A review on performance and emission characteristics of spark ignition engines using methanol as fuel, Energy Rep. 5 (2019) 1025–1035.
[31] Ö. Salih, T. Erdal, D. Usame, E.G. Halil, Thermodynamic, thermoeconomic, and exergoeconomic analysis of a UAV two stroke engine fueled with gasoline-octanol and gasoline-hexanol blends, Energy Convers. Manag. 327 (2025) (2025) 119545.
[32] K. Takei, K. Yoshida, H. Shoji, A. Yamazaki, Combustion analysis of methanol fuel in 2-stroke engine, Proc. JSME Ann. Meet. 4 (2000) 331–332.
[33] S.G. Abed, H.M. Al-Ameri, S.K. Al-Shammari, Exergy analysis of spark-ignition engine fuelled with methanol-gasoline blends, Energy Clim. Change 2 (1) (2022) 1–12.
[34] W. Tutak, A. Jamrozik, M. Pyrc, M. Sosnowski, The impact of engine load on the co-combustion of diesel fuel and bio-oil on performance, combustion and emission characteristics of a CI engine, Sustainability 15 (2) (2023) 1391.
[35] X. Zhu, H. He, L. Kaifa, Z. Peng, Characterizing carbon emissions from China V and China VI gasoline-powered vehicles, J. Clean. Prod. 370 (2022) 133564.
[36] C. Sayin, M. Gumus, M. Canakci, Effect of fuel injection timing on the emissions of a direct injection (DI) diesel engine fueled with methanol–diesel blends, Energy Convers. Manag. 149 (2017) 774–784.
[37] N. Yilmaz, A. Atmanli, F.M. Vigil, Comparative analysis of methanol and ethanol as fuels in compression ignition engines, Renew. Sustain. Energy Rev. 135 (2021) 110239.
[38] A. Atmanli, N. Yilmaz, F.M. Vigil, Evaluation of performance, combustion and emissions in a diesel engine fueled with diesel–biodiesel–alcohol blends, Fuel 158 (2015) 401–409.
[39] S. Özer, A. Arslan, B. Doğan, E. Tunçer, Ö. Arslan, Eco-friendly Nano-Additives: energy, exergy, and environmental impacts in motor vehicle emission control, Int. J. Automot. Sci. Technol. 9 (1) (2025) 121–135.